Temperature dependence of the acentric factor of normal hydrogen, orthohydrogen and parahydrogen

Ramesh A
Arignar Anna Government Arts College
Balasubramanian R (drrbala@yahoo.com)
Arignar Anna Government Arts College

Research Article

Keywords: Acentric factor, Filippov's parameter, normal hydrogen, orthohydrogen, parahydrogen, Riedel parameter

Posted Date: October 17th, 2022

DOI: https://doi.org/10.21203/rs.3.rs-2165775/v1

Temperature dependence of the acentric factor of normal hydrogen, orthohydrogen and parahydrogen

Arumugam Ramesh[a], Ramasamy Balasubramanian[a*]
[a]Department of Physics, Arignar Anna Government Arts College, Namakkal 637002, Tamilnadu, India

[*]Correponding author.
E-mail Address: drrbala@yahoo.com(R. Balasubramanian)
Ph.:+91 9943831176, Fax : 04286-266323

Abstract

Temperature-dependence correlations of vapor pressure and acentric factor for normalhydrogen(n-H_2), orthohydrogen(o-H_2) and parahydrogen(p-H_2), have been formulated. The obtained correlations are statistically excellent. The characteristic parameters such as the Pitzer's acentric factor, Riedel's parameter, Filippov's parameter have been determined for n-H_2, o-H_2 and p-H_2. And, the curvatures of vapor pressure curve for n-H_2, o-H_2 and p-H_2 have been determined in a wide range of temperature. It is found that the curvatures of vapor pressure curve for n-H_2, o-H_2 and p-H_2 have a maximum at about 17.11K, 17.12K and 17.00K, respectively.

Keywords

Acentric factor, Filippov's parameter, normal hydrogen, orthohydrogen, parahydrogen, Riedel parameter

Introduction

Hydrogen(H_2) is a contender for alternative energy. H_2 fuel cell vehicles and H_2 based low-carbon fuels will contribute to the decarbonisation of the mobility sector, shipping and aviation. H_2 is used as a rocket fuel. And, petroleum refining, semiconductor manufacturing, aerospace industry, fertilizer production, metal treatment, pharmaceutical, power plant generator, methanol production, commercial fixation of nitrogen from air, reduction of metallic ores use H_2.

o-H_2 and p-H_2 are nuclear spin isomers of H_2. The nuclear spins of o-H_2 are parallel and that of p-H_2 are antiparallel. They are chemically identical. They have the same atomic and isotopic structure. They differ in the nuclear spin states of their atoms. The energy difference associated with nuclear spin transitions of H_2 is about $0.1 J.mol^{-1}$. However, this tiny change leads to different thermodynamic and spectroscopic properties of H_2 molecules. The o-H_2 and p-H_2 are characterized by different values of specific heat, boiling point and heat of vapor formation. It follows from the Pauli's principle that nuclear spin state and rotational state of the H_2 molecule are correlated. This is attributed to the fact that the molecules of these gases are rotating differently. Conversion between two nuclear spin states of H_2 molecule occurs extremely slowly as the transitions between symmetric and antisymmetric nuclear spin states are forbidden by the selection rule of quantum mechanics. Hence, p-H_2 can be stored as a individual gas for longer periods. However, the use of paramagnetic catalysis promote the establishment of Boltzman's thermodynamic equilibrium between o-H_2 and p-H_2 states for a given temperature at accelerated rate. The paramagnetic materials create a strong inhomogeneous magnetic field at the atomic scale. In such fields, the two H_2 isomers are no longer equivalent. Hence, the spin-flip transitions between o-H_2 and p-H_2 are no longer forbidden. At room temperature, the n-H_2 at thermal equilibrium consists of 75% o-H_2 and 25% p-H_2. Knowledge about o-H_2 to p-H_2 conversion is important for the storage of liquid

H_2. Due to the energy difference associated with different rotational level, energy is released when $o\text{-}H_2$ converts to $p\text{-}H_2$ and energy is absorbed in the reverse process.

The scientific and technical significance has led to numerous experimental and theoretical studies on the thermodynamic properties of H_2[1-14]. The effect of $o\text{-}H_2$ and $p\text{-}H_2$ composition on the performance of a proton exchange membrane fuel cell is calculated and experimentally studied[9]. Equation of state of $o\text{-}H_2$ and $p\text{-}H_2$ has been derived[10]. The influence of $o\text{-}H_2$ and $p\text{-}H_2$ conversion is considered to recommend the parameters for H_2 storage[11]. Sound velocity in liquid $p\text{-}H_2$, dielectric constant of liquid $p\text{-}H_2$ along the saturation line, surface tension of $p\text{-}H_2$ in the temperature range from triple point to critical point and density of liquid $p\text{-}H_2$ along saturation line have been determined[12]. In contrast to bulk metals, the nanoparticles of copper, silver and gold catalyze the low temperature $o\text{-}H_2$ to $p\text{-}H_2$ conversion[14]. $p\text{-}H_2$ is employed in the NMR and MRI signal enhancement[15].

The technological applications of hydrogen require the knowledge of its thermodynamic properties including its acentric factor. Acentric factor is a characteristic thermodynamic parameter of substances. It is a measure of nonsphericity of molecules[16,17]. It accounts[18] for the deviations in the thermodynamic properties of fluids consisting of non-spherical molecules from that of fluids made of spherical molecules. Acentric factor is a used as a parameter in the corresponding state principle[19]. The acentric factor is widely used in determining the thermodynamic properties of substances such as the compressibility factor[20-25], fluid phase equilibrium[26,27], virial coefficients[28,29], vapour pressure[30-32] and enthalpy of vaporization[17,33,34]. Hence, the knowledge of acentric factor of substances acquires significance. In recent years, several studies have been made on the acentric factors of various substances. Acentric factors are correlated[35] to molecular energies of n-alkanes. Artificial neural network group contribution method is used[36] to calculate the acentric factors of pure compounds. The values of acentric factors of limonene and linalool were optimized[37] to improve the performance of the SRE EoS. A new second order group contribution method has been developed[38] to predict the acentric factors of organic compounds. Using the normal boiling temperature, molecular weight and the number of atoms and bonds, empirical correlations are developed[39] to estimate the acentric factors of s-containing compounds. Two different intelligent systems are used to estimate[40] the acentric factors of binary and ternary mixtures of ionic liquids. New generalized models are introduced[41] to estimate the acentric factors of pure compounds. Acentric factors of fluoroalkylsilane compounds have estimated[42] by a group contribution method. Acentric factor of carbon dioxide is required[43] by the cubic equations of state to predict the solid solute solubility in supercritical carbon dioxide. However, the studies on the acentric factors of H_2 and their isomers, particularly their temperature dependence, are scarce.

This work formulates the temperature-dependence correlations for the acentric factor, vapour pressure and the curvature of vapour pressure curve for $n\text{-}H_2$, $o\text{-}H_2$, $p\text{-}H_2$ over a wide range of temperature upto the vicinity of their liquid-vapour critical point.

Vapor pressure

Analysis of the vapour pressure P_{vp} data[44,45] for $n\text{-}H_2$, o-H_2, and $p\text{-}H_2$ shows that its temperature-dependence may be represented by a second degree polynomial. That is,

$$P_{vp} = A_1 + A_2T + A_3T^2 \tag{1}$$

where P_{vp} is in MPa and T is in K.

The coefficients in Eq.(1) are A_1=1.3422, A_2=-0.1560 and A_3=0.0046. The correlation given by Eq.(1) is characterized by the correlation coefficient(R) of 0.9976 and the coefficient of determination(R^2) of 0.9952, respectively. The vapor pressure correlation given by Eq.(1) is depicted in Fig.1 along with the literature data[44,45].

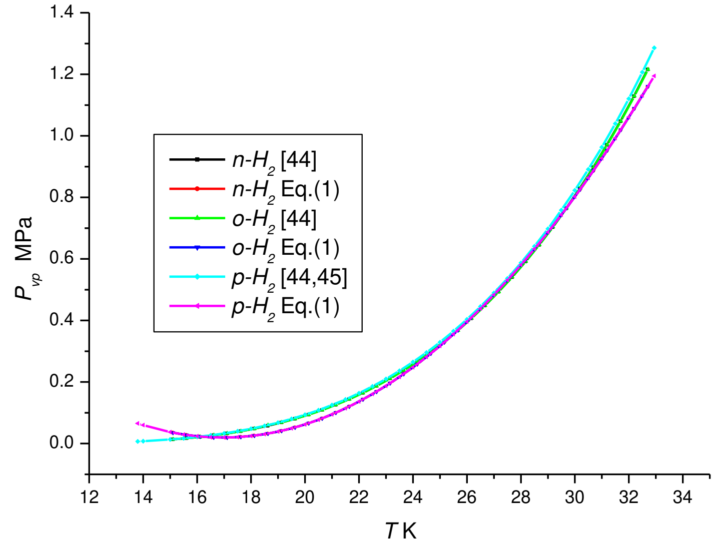

Fig. 1 - Vapour pressure of n-H_2, o-H_2 and p-H_2.

Eq.(1) gives the temperature derivatives of vapour pressure as

$$\frac{dP}{dT} = A_2 + 2A_3T \tag{2}$$

$$\frac{d^2P}{dT^2} = 2A_3 \tag{3}$$

For, n-H_2, o-H_2 and p-H_2, the derivatives dP/dT and d^2P/dT^2 are determined by Eqs.(2) and (3), respectively. The results are presented in the reduced coordinates $T^*=T/T_c$ and $P^*=P/P_c$, in Tables 1-3 and depicted in Fig. 2

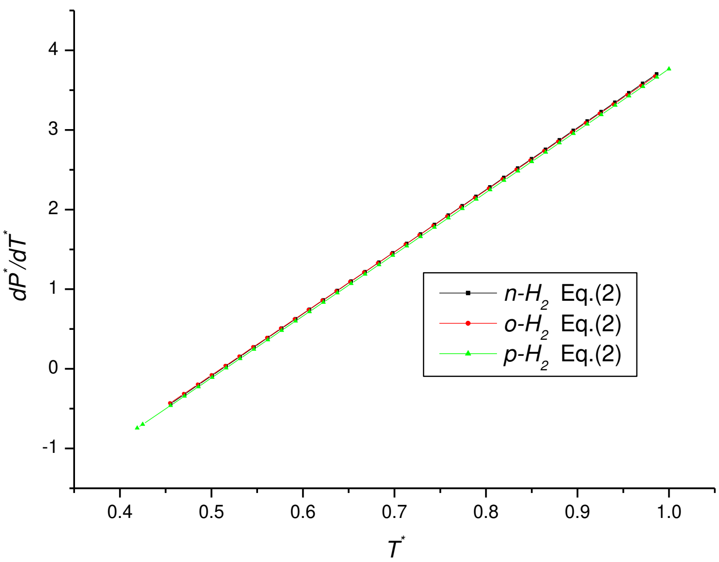

Fig. 2 - dP^*/dT^* versus T^* for n-H_2, o-H_2 and p-H_2.

Curvature of vapor pressure curve

The vapour pressure curve's curvature at a particular temperature is a measure of how the surface bends away from its tangent plane at this point. The curvature of the vapour pressure curve is examined for the proposed P_{vp} correlation. The curvature (inverse of the radius of curvature) of the vapour pressure curve is defined[46] as

$$k = \left(d^2 P^* / dT^{*2}\right)\left[1 + \left(\frac{dP^*}{dT^*}\right)^2\right]^{-3/2} \tag{4}$$

$$\frac{P_c}{T_c}\frac{dP^*}{dT^*} = \frac{dP}{dT} = A_2 + 2A_3 T \tag{5}$$

$$\frac{P_c}{T_c}\frac{d^2P^*}{dT^{2*}} = \frac{d^2P}{dT^2} = 2A_3 \tag{6}$$

For $n\text{-}H_2$, $o\text{-}H_2$ and $p\text{-}H_2$, the curvature k is determined by Eq.(4) using the values of dP/dT and d^2P/dT^2 tabulated in Tables 1-3. The results are also given in Tables 1-3 and depicted in Fig. 3. The curvature of vapour pressure for $n\text{-}H_2$, $o\text{-}H_2$ and $p\text{-}H_2$ is found have a maximum at temperatures $0.5162T_c$, $0.5153T_c$, and $0.5161T_c$, respectively.

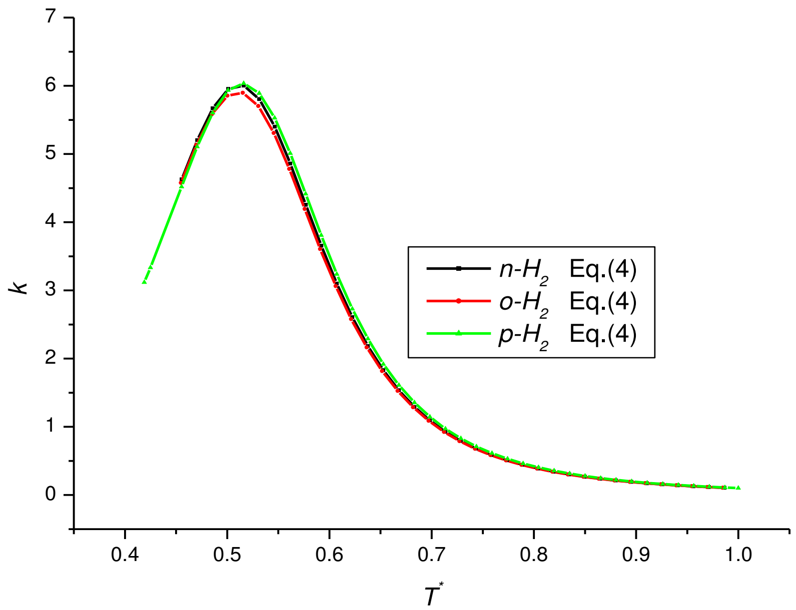

Fig. 3 - Curvature of the vapour pressure curve for $n\text{-}H_2$, $o\text{-}H_2$ and $p\text{-}H_2$.

Table 1 - Curvature of vapour pressure curve k and acentric factor ω of $n\text{-}H_2$.

T^*	dP^*/dT^* Eq.(5)	d^2P^*/dT^{2*} Eq.(6)	k Eq.(4)	ω Eq.(8)	ω Eq.(9)	$d\omega/dT^*$ Eq.(10)	$d^2\omega/dT^{*2}$ Eq.(11)
0.4555	-0.4369	6.0138	4.6272	0.9798	0.941	-5.7761	8.4398
0.4707	-0.3187	6.0138	5.2015	0.8744	0.8544	-5.6481	8.4398
0.4859	-0.2004	6.0138	5.6688	0.7749	0.7697	-5.5201	8.4398
0.5010	-0.0822	6.0138	5.9533	0.6807	0.6869	-5.3921	8.4398
0.5162	0.0361	6.0138	6.0020	0.5915	0.6061	-5.2641	8.4398
0.5314	0.1543	6.0138	5.8052	0.5067	0.5272	-5.1361	8.4398
0.5466	0.2726	6.0138	5.4008	0.4260	0.4503	-5.0080	8.4398

0.5617	0.3908	6.0138	4.8590	0.3492	0.3753	-4.8800	8.4398
0.5769	0.5091	6.0138	4.2561	0.2758	0.3023	-4.7520	8.4398
0.5921	0.6274	6.0138	3.6555	0.2056	0.2311	-4.6240	8.4398
0.6072	0.7456	6.0138	3.0986	0.1384	0.162	-4.4960	8.4398
0.6224	0.8639	6.0138	2.6060	0.0740	0.0948	-4.3679	8.4398
0.6376	0.9821	6.0138	2.1840	0.0122	0.0295	-4.2399	8.4398
0.6527	1.1004	6.0138	1.8294	-0.0472	-0.0339	-4.1119	8.4398
0.6679	1.2186	6.0138	1.5351	-0.1044	-0.0953	-3.9839	8.4398
0.6831	1.3369	6.0138	1.2923	-0.1595	-0.1547	-3.8559	8.4398
0.6982	1.4551	6.0138	1.0926	-0.2126	-0.2122	-3.7279	8.4398
0.7134	1.5734	6.0138	0.9281	-0.2639	-0.2678	-3.5998	8.4398
0.7286	1.6916	6.0138	0.7925	-0.3135	-0.3214	-3.4718	8.4398
0.7437	1.8099	6.0138	0.6802	-0.3615	-0.3731	-3.3438	8.4398
0.7589	1.9282	6.0138	0.5869	-0.4079	-0.4229	-3.2158	8.4398
0.7741	2.0464	6.0138	0.5089	-0.4529	-0.4707	-3.0878	8.4398
0.7892	2.1647	6.0138	0.4436	-0.4966	-0.5165	-2.9598	8.4398
0.8044	2.2829	6.0138	0.3884	-0.5390	-0.5605	-2.8317	8.4398
0.8196	2.4012	6.0138	0.3417	-0.5802	-0.6025	-2.7037	8.4398
0.8347	2.5194	6.0138	0.3019	-0.6203	-0.6425	-2.5757	8.4398
0.8499	2.6377	6.0138	0.2679	-0.6593	-0.6806	-2.4477	8.4398
0.8651	2.7559	6.0138	0.2386	-0.6973	-0.7168	-2.3197	8.4398
0.8803	2.8742	6.0138	0.2134	-0.7343	-0.751	-2.1916	8.4398
0.8954	2.9925	6.0138	0.1915	-0.7705	-0.7832	-2.0636	8.4398
0.9106	3.1107	6.0138	0.1724	-0.8058	-0.8136	-1.9356	8.4398
0.9258	3.2290	6.0138	0.1557	-0.8404	-0.842	-1.8076	8.4398
0.9409	3.3472	6.0138	0.1411	-0.8742	-0.8684	-1.6796	8.4398
0.9561	3.4655	6.0138	0.1282	-0.9074	-0.8929	-1.5516	8.4398
0.9713	3.5837	6.0138	0.1168	-0.9400	-0.9155	-1.4235	8.4398
0.9864	3.7020	6.0138	0.1066	-0.9721	-0.9361	-1.2955	8.4398

Table 2 - Curvature of vapour pressure curve *k* and acentric factor *ω* of *o-H₂*.

T^*	dP^*/dT^* Eq.(5)	d^2P^*/dT^{2*} Eq.(6)	k Eq.(4)	ω Eq.(8)	ω Eq.(9)	$d\omega/dT^*$ Eq.(10)	$d^2\omega/dT^{*2}$ Eq.(11)
0.4548	-0.4311	5.9104	4.5770	0.9845	0.9454	-5.7825	8.4398
0.4699	-0.3138	5.9104	5.1337	0.8792	0.8588	-5.6548	8.4398
0.4851	-0.1965	5.9104	5.5837	0.7797	0.7742	-5.5270	8.4398
0.5002	-0.0793	5.9104	5.8551	0.6856	0.6915	-5.3992	8.4398
0.5153	0.0380	5.9104	5.8976	0.5964	0.6107	-5.2715	8.4398
0.5305	0.1553	5.9104	5.7029	0.5116	0.5319	-5.1437	8.4398
0.5456	0.2725	5.9104	5.3081	0.4310	0.455	-5.0159	8.4398
0.5608	0.3898	5.9104	4.7804	0.3396	0.38	-4.8882	8.4398
0.5759	0.5071	5.9104	4.1932	0.2807	0.307	-4.7604	8.4398
0.5910	0.6243	5.9104	3.6073	0.2105	0.2359	-4.6326	8.4398
0.6062	0.7416	5.9104	3.0628	0.1433	0.1667	-4.5049	8.4398
0.6213	0.8589	5.9104	2.5803	0.0789	0.0995	-4.3771	8.4398
0.6364	0.9761	5.9104	2.1658	0.0170	0.0342	-4.2494	8.4398
0.6516	1.0934	5.9104	1.8168	-0.0425	-0.0291	-4.1216	8.4398
0.6667	1.2107	5.9104	1.5265	-0.0997	-0.0906	-3.9938	8.4398
0.6819	1.3279	5.9104	1.2866	-0.1549	-0.1501	-3.8661	8.4398
0.6970	1.4452	5.9104	1.0888	-0.2081	-0.2076	-3.7383	8.4398

0.7121	1.5625	5.9104	0.9258	-0.2594	-0.2632	-3.6105	8.4398
0.7273	1.6797	5.9104	0.7911	-0.3091	-0.3169	-3.4828	8.4398
0.7424	1.7970	5.9104	0.6795	-0.3571	-0.3687	-3.3550	8.4398
0.7575	1.9143	5.9104	0.5867	-0.4036	-0.4185	-3.2272	8.4398
0.7727	2.0315	5.9104	0.5091	-0.4487	-0.4664	-3.0995	8.4398
0.7878	2.1488	5.9104	0.4439	-0.4924	-0.5124	-2.9717	8.4398
0.8030	2.2661	5.9104	0.3889	-0.5348	-0.5564	-2.8439	8.4398
0.8181	2.3834	5.9104	0.3423	-0.5760	-0.5985	-2.7162	8.4398
0.8332	2.5006	5.9104	0.3026	-0.6161	-0.6386	-2.5884	8.4398
0.8484	2.6179	5.9104	0.2686	-0.6552	-0.6768	-2.4606	8.4398
0.8635	2.7352	5.9104	0.2393	-0.6932	-0.7131	-2.3329	8.4398
0.8787	2.8524	5.9104	0.2140	-0.7302	-0.7475	-2.2051	8.4398
0.8938	2.9697	5.9104	0.1921	-0.7663	-0.7799	-2.0773	8.4398
0.9089	3.0870	5.9104	0.1730	-0.8016	-0.8104	-1.9496	8.4398
0.9241	3.2042	5.9104	0.1563	-0.8361	-0.8389	-1.8218	8.4398
0.9392	3.3215	5.9104	0.1416	-0.8699	-0.8655	-1.6940	8.4398
0.9543	3.4388	5.9104	0.1287	-0.9030	-0.8902	-1.5663	8.4398
0.9695	3.5560	5.9104	0.1173	-0.9355	-0.9129	-1.4385	8.4398
0.9846	3.6733	5.9104	0.1071	-0.9674	-0.9337	-1.3107	8.4398

Table 3 - Curvature of vapor pressure curve *k* and acentric factor *ω* of *p-H₂*.

T^*	dP^*/dT^* Eq.(5)	d^2P^*/dT^{2*} Eq.(6)	k Eq.(4)	ω Eq.(8)	ω Eq.(9)	$d\omega/dT^*$ Eq.(10)	$d^2\omega/dT^{*2}$ Eq.(11)
0.4190	-0.7439	6.0372	3.1182	1.2615	1.1579	-6.0848	8.4398
0.4250	-0.6968	6.0372	3.3345	1.2124	1.1211	-6.0335	8.4398
0.4554	-0.4611	6.0372	4.5212	0.9804	0.9418	-5.7773	8.4398
0.4706	-0.3433	6.0372	5.1082	0.8748	0.8551	-5.6492	8.4398
0.4858	-0.2254	6.0372	5.6046	0.7752	0.7703	-5.5211	8.4398
0.5009	-0.1076	6.0372	5.9339	0.6809	0.6875	-5.3930	8.4398
0.5161	0.0102	6.0372	6.0362	0.5916	0.6066	-5.2648	8.4398
0.5313	0.1281	6.0372	5.8916	0.5067	0.5277	-5.1367	8.4398
0.5465	0.2459	6.0372	5.5282	0.4260	0.4507	-5.0086	8.4398
0.5617	0.3638	6.0372	5.0105	0.3491	0.3756	-4.8805	8.4398
0.5768	0.4816	6.0372	4.4152	0.2756	0.3025	-4.7524	8.4398
0.5920	0.5994	6.0372	3.8094	0.2054	0.2313	-4.6243	8.4398
0.6072	0.7173	6.0372	3.2392	0.1382	0.1621	-4.4961	8.4398
0.6224	0.8351	6.0372	2.7300	0.0738	0.0948	-4.3680	8.4398
0.6376	0.9529	6.0372	2.2905	0.0120	0.0295	-4.2399	8.4398
0.6527	1.0708	6.0372	1.9196	-0.0475	-0.0339	-4.1118	8.4398
0.6679	1.1886	6.0372	1.6108	-0.1046	-0.0954	-3.9837	8.4398
0.6831	1.3065	6.0372	1.3556	-0.1598	-0.1549	-3.8556	8.4398
0.6983	1.4243	6.0372	1.1454	-0.2129	-0.2124	-3.7274	8.4398
0.7135	1.5421	6.0372	0.9723	-0.2642	-0.268	-3.5993	8.4398
0.7286	1.6600	6.0372	0.8295	-0.3138	-0.3217	-3.4712	8.4398
0.7438	1.7778	6.0372	0.7114	-0.3618	-0.3734	-3.3431	8.4398
0.7590	1.8956	6.0372	0.6132	-0.4082	-0.4232	-3.2150	8.4398
0.7742	2.0135	6.0372	0.5313	-0.4532	-0.471	-3.0869	8.4398
0.7894	2.1313	6.0372	0.4627	-0.4969	-0.5169	-2.9587	8.4398
0.8045	2.2491	6.0372	0.4048	-0.5393	-0.5608	-2.8306	8.4398
0.8197	2.3670	6.0372	0.3558	-0.5805	-0.6028	-2.7025	8.4398

0.8349	2.4848	6.0372	0.3142	-0.6206	-0.6429	-2.5744	8.4398
0.8501	2.6027	6.0372	0.2785	-0.6596	-0.681	-2.4463	8.4398
0.8653	2.7205	6.0372	0.2479	-0.6976	-0.7172	-2.3182	8.4398
0.8804	2.8383	6.0372	0.2215	-0.7346	-0.7514	-2.1900	8.4398
0.8956	2.9562	6.0372	0.1986	-0.7708	-0.7837	-2.0619	8.4398
0.9108	3.0740	6.0372	0.1787	-0.8061	-0.814	-1.9338	8.4398
0.9260	3.1918	6.0372	0.1613	-0.8407	-0.8424	-1.8057	8.4398
0.9412	3.3097	6.0372	0.1461	-0.8745	-0.8688	-1.6776	8.4398
0.9563	3.4275	6.0372	0.1326	-0.9077	-0.8933	-1.5495	8.4398
0.9715	3.5454	6.0372	0.1208	-0.9403	-0.9158	-1.4213	8.4398
0.9867	3.6632	6.0372	0.1103	-0.9724	-0.9364	-1.2932	8.4398
1.0000	3.7664	6.0372	0.1020	-1.0001	-0.9529	-1.1810	8.4398

Acentric factor

Pitzer's acentric factor ω_P is defined[47] such that its value is zero for spherical molecules. That is,

$$\omega_P = -1 - \log_{10}(P^*_{vp}\ \ at\ \ T^* = 0.7) \tag{7}$$

where $P^*_{vp} = P_{vp} / P_c$.

On the other hand, the acentric factor ω being a measure of deviation in the properties of nonspherical molecules from that of spherical molecules. This deviation depends on temperature. Hence, Eq.(7) may be generalized to get the temperature-dependent acentric factor as

$$\omega(T) = -1 - \log_{10}(P^*_{vp}) \tag{8}$$

Using the data on P^*_{vp} obtained by the correlation given by Eq.(1) for *n-H*$_2$, *o-H*$_2$ and *p-H*$_2$, their acentric factors are calculated by Eq.(8). The results are presented in Tables 1-3 and depicted in Fig. 4

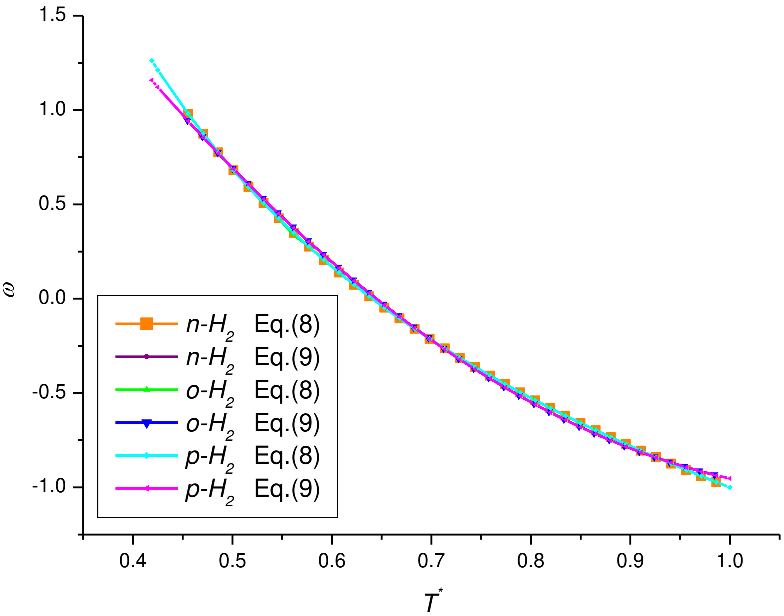

Fig. 4 - Acentric factor of *n-H*$_2$, *o-H*$_2$ and *p-H*$_2$.

For $n\text{-}H_2$, $o\text{-}H_2$ and $p\text{-}H_2$, the values of ω may be fitted to a second degree polynomial in temperature. That is,

$$\omega = B_1 + B_2 T^* + B_3 T^{*2} \tag{9}$$

The coefficients in Eq.(1) are B_1 = 4.4480, B_2 = -9.6208 and B_3 = 4.2199. The correlation given by Eq.(9) is characterized by the correlation coefficient(R) of 0.9992 and the coefficient of determination(R^2) of 0.9985, respectively.

Eq.(9) gives the temperature derivatives of acentric factor as

$$\frac{d\omega}{dT^*} = B_2 + 2B_3 T^* \tag{10}$$

$$\frac{d^2\omega}{dT^{*2}} = 2B_3 \tag{11}$$

For $n\text{-}H_2$, $o\text{-}H_2$ and $p\text{-}H_2$, the derivatives $d\omega/dT^*$ and $d^2\omega/dT^{*2}$ are determined by Eq.(10) and (11), respectively. The results are presented in Tables 1-3 and depicted in Fig.5

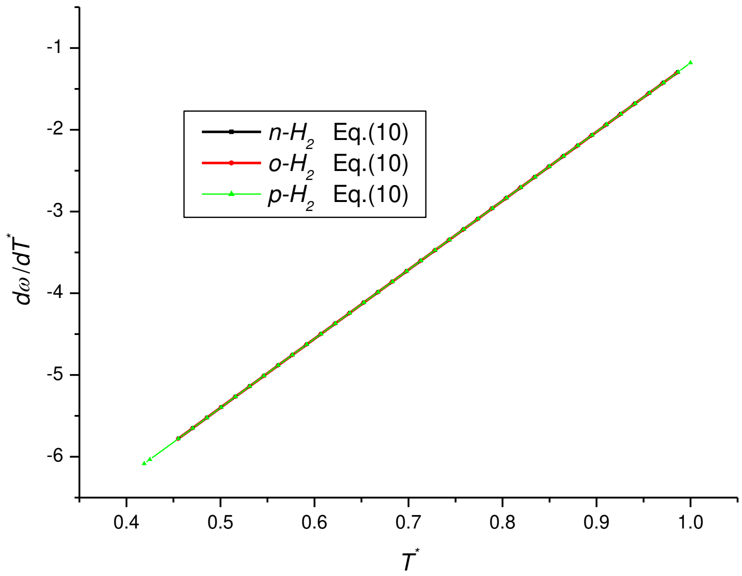

Fig. 5 - $d\omega/dT^*$ versus T^* for $n\text{-}H_2$, $o\text{-}H_2$ and $p\text{-}H_2$.

Riedel's parameter

Riedel's parameter α_R is a measure of the temperature-dependence of vapour pressure in the vapour-liquid critical region. It determines the slope of the fluid-phase equilibrium curve in the critical region. The Riedel's parameter α_R is correlated[48] to the Pitzer's acentric factor ω_P by

$$\alpha_R = 4.919\omega_P + 5.811 \tag{12}$$

Pitzer's acentric factor ω_p and Riedel's parameter α_R for n-H_2, o-H_2 and p-H_2 are determined by Eqs.(7) and (12). The obtained values are given in Table 4. For comparison, the values of ω_p and α_R calculated through other correlations are also presented in Table 4.

Table 4 - The Pitzer's acentric factor and the Riedel's parameter for n-H_2, o-H_2 and p-H_2.

Correlation	ω_p			α_R Eq.(12)		
	n-H_2	o-H_2	p-H_2	n-H_2	o-H_2	p-H_2
This Work	-0.2170	-0.2175	-0.2220	4.7438	4.7411	4.7191
Brandani (B.II)[52]	-0.2565	-0.2497	-0.2511	4.5493	4.5830	4.5757
Empirical correlation[49]	-0.2565	-0.2491	-0.2506	4.5494	4.5856	4.5783
Edmister[49]	-0.2502	-0.2427	-0.2442	4.5803	4.6169	4.6096
Brandani (B.I)[52]	-0.2447	-0.2382	-0.2397	4.6074	4.6392	4.6320
Ambrose-Walton(II)[52]	-0.2287	-0.2222	-0.2240	4.6859	4.7179	4.7092
CSGC-Reidel Equation[50]	-0.2270	-0.2204	-0.2221	4.6946	4.7267	4.7184
Lee-Kesler[49]	-0.2242	-0.2178	-0.2195	4.7082	4.7398	4.7314
Twu et al.[52]	-0.2232	-0.2169	-0.2187	4.7131	4.7442	4.7353
Ambrose-Walton(I)[51]	-0.2098	-0.2037	-0.2053	4.7789	4.8089	4.8011

To evaluate the performance characteristics of Eqs.(11) and (12), percentage errors in the Pitzer's acentric factor and the Riedel's parameter determined in this work compared to other correlations are given in Table 5.

Table 5 –Percentage error in the Pitzer's acentric factor and the Riedel's parameter.

Correlation for comparison	Percentage error% in ω_p			Percentage error% in α_R		
	n-H_2	o-H_2	p-H_2	n-H_2	o-H_2	p-H_2
Brandani (B.II)[52]	12.8793	15.4144	11.6135	-3.4511	-4.2748	-3.1354
Empirical correlation[49]	12.6908	15.4128	11.4268	-3.3913	-4.2743	-3.0768
Edmister[49]	10.4002	13.2834	9.1203	-2.6898	-3.5690	-2.3771
Brandani (B.I)[52]	8.6964	11.3331	7.3907	-2.1965	-2.9605	-1.8812
Ambrose-Walton(II)[52]	2.1259	5.1483	0.8980	-0.4926	-1.2361	-0.2101
CSGC-Reidel Equation[50]	1.3344	4.4119	0.0694	-0.3061	-1.0492	-0.0161
Lee-Kesler[49]	0.1191	3.2273	-1.1389	-0.0269	-0.7559	0.2599
Twu et al.[52]	-0.2874	2.7956	-1.5008	0.0646	-0.6512	0.3409
Ambrose-Walton(I)[51]	-6.7681	-3.3988	-8.1186	1.4103	0.7340	1.7077

Filippov's parameter

Filippov's parameter α_F is another measure of the temperature-dependence of vapour pressure in the vapour-liquid critical region. It is defined[48] by

$$\alpha_F = 100 \times P_{vp}^{*} (at\ T^{*} = 0.625) \tag{13}$$

Filippov's parameter for n-H_2, o-H_2 and p-H_2 are determined by Eq. (13). And its value for n-H_2, o-H_2 and p-H_2 is 7.2909, 7.3207 and 7.0853, respectively.

Correlations between $\omega_P, \alpha_R, \alpha_F$ and the critical compressibility factor Z_c

The correlations between various characteristic parameters of substances are of significance due to their ability to predict their properties and to reveal the underlying theory. In this respect, Pitzer's acentric factor, Riedel's parameter, Filippov's parameter for *n*-H_2, *o*-H_2 and *p*-H_2 obtained in this work and the critical compressibility factor[53-58] are shown in Figs. 6a, 6b, 6c, 6d and 6e.

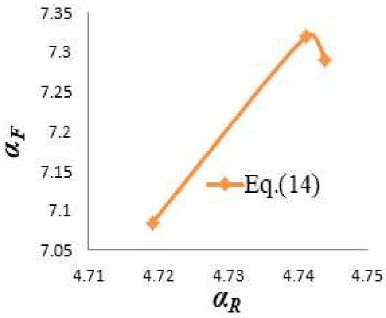

Fig.6a - α_F versus α_R

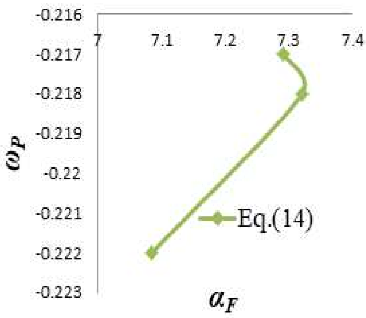

Fig.6b - ω_P versus α_F

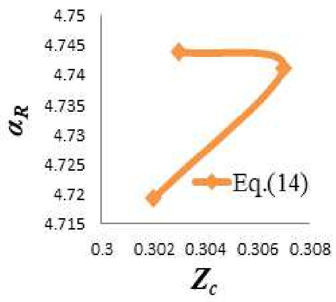

Fig.6c - α_R versus Z_c[53-58]

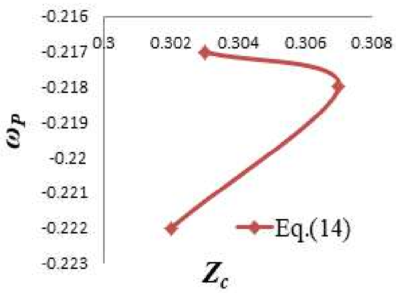

Fig.6d - ω_P versus Z_c [53-58]

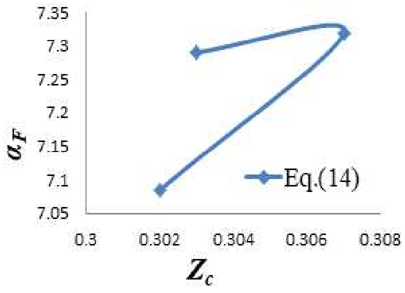

Fig.6e - α_F versus Z_c [53-58]

As seen, these parameters for *n*-H_2, *o*-H_2 and *p*-H_2 may be correlated by a second degree polynomial of the form:

$$Y = a_0 + a_1 X + a_2 X^2 \qquad (14)$$

Where X and Y are characteristic parameters such as ω_p, α_R, α_F and Z_c. The coefficients in Eq.(14) are presented in Table 6.

Table 6 - The coefficients in Eq.(14).

X	Y	a_0	a_1	a_2	R	R^2
α_R	α_F	-19733.2	8336.07	-880.042	0.9999	0.9998
α_F	ω_p	-13.0951	3.5589	-0.2459	0.9999	0.9998
Z_c	α_R	-3681.39	24181.7	-39630	0.9999	0.9998
Z_c	ω_p	-97.8133	640.25	-1050	0.9999	0.9998
Z_c	α_F	-467.133	3095.08	-5075	0.9999	0.9998

And, the ratios α_F / α_R and α_F / ω_P for n-H_2, o-H_2 and p-H_2 are presented in Table 7.

Table 7 - α_F / α_R and α_F / ω_P for n-H_2, o-H_2 and p-H_2.

Parameter	n-H_2	o-H_2	p-H_2
$\frac{\alpha_F}{\alpha_R}$	1.5369	1.5441	1.5014
$\frac{\alpha_F}{\omega_p}$	-33.5986	-33.5812	-31.9158

Results and analysis

Eq.(1) and Fig.1 reveal that the vapor pressure of n-H_2, o-H_2 and p-H_2 has a parabolic dependence on temperature. This vapor pressure correlation is characterized by the correlation coefficient R of 0.9976 and the coefficient determination R^2 of 0.9952. That's the, the vapor pressure-temperature correlation formulated in this work is excellent from the statistical consideration. Hence, this correlation may be used as a basis for determining other thermodynamic properties of n-H_2, o-H_2 and p-H_2. Based on Eq.(1), the acentric factors of n-H_2, o-H_2 and p-H_2 have been determined over a wide range of temperature. It is shown that the temperature dependence of the acentric factor for n-H_2, o-H_2 and p-H_2 may be represented by a second degree polynomial with the correlation coefficient R of 0.9992 and the coefficient determination R^2 of 0.9985. Thus, the acentric factor correlation given by Eq.(7) is an excellent one from the statistical view point.

The Pitzer's acentric factors for n-H_2, o-H_2 and p-H_2 are found to be -0.2170, -0.2175 and -0.2220, respectively. The percentage errors in the obtained values of the Pitzer's acentric factor of n-H_2, o-H_2 and p-H_2 compared to that of other known correlations[49-52] are in the range of about 0.07% to 15%. That is, the correlation given by Eq. (9) reliably accommodates the Pitzer's acentric factors of n-H_2, o-H_2 and p-H_2 from the literature[49-52]. The values of the Riedel's parameters for n-H_2, o-H_2 and p-H_2 are 4.7438, 4.7411 and 4.7191, respectively. The percentage errors in the obtained values of the Riedel's parameter of n-H_2, o-H_2 and p-H_2 compared to that of other known correlations[49-52] are in the range of about -0.02% to -4.28%. The values of the Filippov's parameter for n-H_2, o-H_2 and p-H_2 are found to be 7.2909, 7.3207 and 7.0853, respectively. The ratio of the Filippov's parameter to the Riedel's parameter for n-H_2, o-H_2 and p-H_2 is about 1.53, 1.54 and 1.50, respectively. And, the ratio of the Filippov's parameter to the Pizter's acentric factor for n-H_2, o-H_2 and p-H_2 is about -33.03,-33.58 and -31.92, respectively. As seen from Eq.(14) and Table 6, the Pitzer's acentric factor, Riedel's parameter, Filippov's parameter and the critical compressibility factor of n-H_2, o-H_2 and p-H_2 may be correlated by a second degree polynomial. For n-H_2, o-H_2 and p-H_2, the curvature of the vapor pressure curve is found to have a maximum at 17.11K, 17.12K and 17.00K, respectively.

Conclusion

Temperature-dependence correlations of vapor pressure and acentric factor for n-H_2, o-H_2 and p-H_2, have been formulated. The obtained correlations are statistically excellent. The characteristic parameters such as the Pitzer's acentric factor, Riedel's parameter, Filippov's parameter have been determined for n-H_2, o-H_2 and p-H_2. And, the curvatures of vapor pressure curve for n-H_2, o-H_2 and p-H_2 have been determined in a wide range of temperature.

It is found that the curvatures of vapor pressure curve for $n\text{-}H_2$, $o\text{-}H_2$ and $p\text{-}H_2$ have a maximum at about 17.11K, 17.12K and 17.00K, respectively.

Reference

[1] Momirlan M, Veziroglu T. The properties of hydrogen as fuel tomorrow in Sustainable energy system for a cleaner planet. Inter J of Hydrogen Energy. 2005; 30(7): 795–802. doi:10.1016/j.ijhydene.2004.10.

[2] Jain IP. Hydrogen the fuel for 21st century. Inter J of Hydrogen Energy. 2009; 34(17): 7368–7378. doi:10.1016/j.ijhydene2009.05.0930.

[3] Ball M, Wietschel M. The future of hydrogen – opportunities and Challenges. Inter J of Hydrogen Energy. 2009;34(2):615–627. doi:10.1016/j.ijhydene.2008.11.

[4] Cecere D, Giacomazzi E, Ingenito A. A review on hydrogen industrial aerospace applications. Inter J of Hydrogen Energy. 2014;39(20):10731–10747. https://doi.org/ 10.1 016 /j.ijhydene.2014.04.126.

[5] Okolie JA, Patra BR, Mukherjee A, Nanda S, Dalai AK, Kozinski JA. Futuristic applications of hydrogen in energy, biorefining, aerospace, pharmaceuticals and metallurgy. Inter J of Hydrogen Energy. 2021;46(13):8885–8905. doi:10.1016/j.ijhyd ene.2021.01.

[6] Yue M, Lambert H, Pahon E, Roche R, Jemei S, Hissel D. Hydrogen energy systems: A critical review of technologies, applications, trends and challenges. Renewable and Sustainable Energy Reviews. 2021;146:111180. doi:10.1016/j.rser. 2021.111180.

[7] Abohamzeh E, Salehi F, Sheikholeslami M, Abbassi R, Khan F. Review of hydrogen safety during storage, transmission, and applications processes. J of Loss Prevention in the Process Industries. 2021; 72: 104569. doi:10.1016/j.jlp.2021.104569.

[8] Liu W, Zuo H, Wang J, Xue Q, Ren B, Yang F. The production and application of hydrogen in steel industry. Inter J of Hydrogen Energy. 2021;46(17): 10548–10569. doi:10.1016/ j.ijhydene.2020.12.

[9] Bahrami J, Gavin P, Bliesner R, Ha S, Pedrow P, Sani AM-, Leachman J. Effect of orthohydrogen–parahydrogen composition on performance of a proton exchange membrane fuel cell. Inter J of Hydrogen Energy. 2014;39(27):14955–14958. doi:10.1016/j.ij hydene.2014.07.

[10] Valenti G, Macchi E, Brioschi S. The influence of the thermodynamic model of equilibrium-hydrogen on the simulation of its liquefaction. Inter J of Hydrogen Energy. 2012;37(14):10779–10788. doi:10.1016/j.ijhydene.2012.04.

[11] Yanxing Z, Maoqiong G, Yuan Z, Xueqiang D, Jun S. Thermodynamics analysis of hydrogen storage based on compressed gaseous hydrogen, liquid hydrogen and cryo-compressed hydrogen. Inter J of Hydrogen Energy. 2019. doi:10.1016/j.ijhydene. 2019.04.207.

[12] Podgorny AN, Pashkor VV. Peculiarites of thermodynamic behaviour of liquid hydrogen. Inter J Hydrogen Energy. 1988;13(4):231-237. https://doi.org/10.1016/0360-3199(88)90090-0.

[13] SherwinJA. Scattering of slow twisted neutron by orthohydrogen and Parahydrogen. Physics letters A. 2022;437:128102.10.1016/j.physleta.2022.128102.

[14] Boeva O, Antonov A, Zhavoronkova K. Influence of the nature of IB group metals on catalytic activity in reactions of homomolecular hydrogen exchange on Cu, Ag, Au nanoparticles. Catalysis Communications. 2021;148:106173. doi:10.1016/j.catcom.2 020.106173.

[15] Kovtunov KV. Koptyug IV, Fekete M, Duckett SB, Theis T, Joalland B, Chekmenev EY. Parahydrogen- Induced Hyperpolarization of Gases. Angewandte Chemie International Edition. 2020; 59(41):17788–17797.doi:10.1002/anie.201915306.

[16] Pitzer KS. The Volumetric and Thermodynamic Properties of Fluids. I. Theoretical Basis and Virial Coefficients. J Am Chem Soc. 1955; 77(13):3427–3433. https://doi.org/10.1021/ja01618a001.

[17] Pitzer KS, Lippman DZ, Curl RF, Huggins CM, Petersen DE. The Volumetric and Thermodynamic Properties of Fluids. II. Compressibility Factor, Vapor Pressure and Entropy of Vaporization. J Am Chem Soc. 1955;77(13)3433–3440. https://doi.org/10.1021/ja01618a002.

[18] Saville G. Acentric Factor. A-to-Z Guide to Thermodynamics, Heat and Mass Transfer, and Fluids Engineering.2006; doi:10.1615/AtoZ.a.acentric_factor.

[19] Bouta A, Colina C, Fuentes MO-. Parameterization of molecular-based equations of state. Fluid phase Equilibria. 2005; 228–229:561–575. doi:10.1016/j.fluid.2004.08.043.

[20] Edmister WC. Applied Hydrocarbon Thermodynamics(Part 4). Petrol Refiner.1958; 37:4.173-179. JST Material Number： D0303A.

[21] Leland TW, Chappelear PS. The corresponding states principle—a review of current theory and practice. Ind Eng Chem. 1968; 60(7):15–43. https://doi.org/10.1021/ie50703a005.

[22] Fisher GD, Jr TWL. Corresponding States Principle Using Shape Factors. Ind Eng Chem Fundam.1970;9(4):537–544. https://doi.org/10.1021/i160036a003.

[23] Stiel LI. A generalized theorem of corresponding states for the thermodynamic properties of nonpolar and polar fluids. Chem Eng Sci. 1972;27(12):2109-2116. https://doi.org/10.1016/0009-2509(72)85090-5.

[24] Teja AS. A Corresponding States equation for saturated liquid densities. I. Applications to LNG. AIChE J. 1980;26:337. https://doi.org/10.1002/aic.690260302.

[25] Wu GZA, Stiel LI, A generalized equation of state for the thermodynamic properties of polar fluids. AIChE J. 1985;31:1632. https://doi.org/10.1002/aic.690311007.

[26] Bhirud VL. A four-parameter corresponding states theory: Saturated liquid densities of anormal fluids. AIChE J. 1978; 24(5):800-885.https://doi.org/10.1002/aic.690240514.

[27] Bhirud VL. Saturated liquid densities of normal fluids, AIChE J. 1978;24(6): 1127-1131. https://doi.org/10.1002/aic.690240630.

[28] Tsonopoulos C. An empirical correlation of second virial coefficients. AIChE J. 1974; 20:263. https://doi.org/10.1002/aic.690200209.

[29] Ness HCV, Abbott MM. Classical Thermodynamics of Nonelectrolyte Solutions. McGraw–Hill. New York; 1982.126–133.

[30] Armstrong B. Saturation properties of chlorine by the principle of corresponding states. J Chem Eng Data.1981;26(2):161-168. https://doi.org/10.1021/je00024a023.

[31] Teja AS, Sandler SI, Patel NC. A generalization of the corresponding states principle using two nonspherical reference fluids. Chem Eng J.1981; 21(1):21-28. https://doi.org/10.1016/0300-9467(81)80053-6.

[32] Lee J.-Y. A semi-empirical vapor pressure equation derived from the van der Waals equation. Fluid Phase Equilibria. 2022; 556:113365. https://doi.org/10.1016/j.fluid.2021.113365.

[33] Nath J. Acentric Factor and the Heats of Vaporization for Unassociated Polar and Nonpolar Organic Liquids. Ind Eng Chem Fundam. 1979; 18(3):297-298. https://doi.org/10.1021/i160071a020.

[34] Sudip D, Ayesha P, Sanjay MM. Saturated Vapor Pressure, Critical State Parameters and Vaporization Enthalpy of 2-Phenyloxirane. Fluid Phase Equilibria. 2020; 112892. doi:10.1016/j.fluid.2020.112892

[35] Machín I, Fuentes C. O-. Interpretation and correlation of acentric factors in terms of Molecular energies, J of Computational Methods in Sci. and Engi. 2017;17(1):161–175. doi:10.3233/JCM-160670.
[36] Gharagheizi F, Eslamimanesh A, Mohammadi AH, Richon D. Determination of Critical Properties and Acentric Factors of Pure Compounds Using the Artificial Neural Network Group Contribution Algorithm. J Chem Eng Data. 2011;56(5): 2460–2476. dx.doi.org/10.1021/je200019g.
[37] Raeissi S, Diaz S, Espinosa S, Peters CJ, Brignole EA. Ethane as an alternative solvent for supercritical extraction of orange peel oils. The J of Supercritical Fluids. 2008;45(3):306–313. https://doi.org/10.1016/j.supflu.2008.01.008.
[38] Saba T, Habib G, Kamyar M. Estimation of the acentric factor of organic compounds via a new group contribution method. Fluid Phase Equilibria. 2019; 499: 112246. doi:10.1016/j.fluid.2019.112246.
[39] Ghomisheh Z, Sobati MA, Gorji AE. New empirical correlations for the prediction of critical properties and acentric factor of S-containing compounds. J of Sulfur Chem. 2022;43(3):327-351. https://doi.org/10.1080/17415993.2021.2017936.
[40] Teslim O, Oghenerume O, Falola Y. Modeling the acentric factor of binary and ternary mixtures of ionic liquids using advanced intelligent systems. Fluid Phase Equilibria. 2020;516:112587. https://doi.org/10.1016/j.fluid.2020.112587.
[41] Abdolhossein H-S, Ameli F, Varamesh A, Shamshirband S, Mohammadi AH, Dabir B, Toward generalized models for estimating molecular weights and acentric factors of pure chemical compounds, Inter J of Hydrogen Energy, 2018;43(5):2699-2717. doi:10.1016/j.ijhydene.2017.12.029.
[42] Pan J, Hong D, Wengeng L, Daowei C, Yunfeng Z, Liangbing H, Zhirong Q, Chuan W. Measurement and correlation of the saturated vapor pressures of Ethenyltris(2,2,2-trifluoroethoxy)silane, Dimethoxymethyl(3,3,3-trifluoropropyl)silane and Trimethoxy(3,3,3-trifluoropropyl)silane. Fluid Phase Equilibria. 2020;509:112457. https://doi.org/10.1016/j.fluid.2020.112457.
[43] Wang H-W, Hsieh C-M. Prediction of solid solute solubility in supercritical carbon dioxide from PSRK EOS with only input of molecular structure. The J of Supercritical Fluids. 2022;180,105446. https://doi.org/10.1016/J.SUPFLU. 2021.105446.
[44] Leachman JW, Jacobsen RT, Penoncello SG, Lemmon EW. Fundamental Equations of State for Parahydrogen, Normal Hydrogen, and Orthohydrogen. J Phys Chem Ref Data. 2009;38(3):721. https://doi.org/10.1063/1.3160306.
[45] Haynes WM, Lide DR, Bruno TJ, CRC Handbook of Chemistry and Physics 95th Edition, A Ready-Reference Book of Chemical and Physical Data.CRC Press, Taylor & Francis Group, 6000 Broken Sound Parkway NW, Suite 300,Boca Raton, FL 33487-2742; 2014.
[46] Srinivasan K. Curvature of the vapour pressure curve. Chem Eng J. 2001;81(1-3)63-67. https://doi.org/10.1016/S1385-8947(00)00223-0.
[47] Reid RC, Prausnitz JM, Poling BE. The Properties of Gases and Liquids. 4th Edition. McGraw–Hill. New York. 1988;23.
[48] Filippov LP. Estimation of Thermophysical Propertics of Liquids and Gases. Energoatomizdat. Moscow. 1988;55.
[49] Chen DH, Dinivahi MV, Jeng C-Y. New Acentric Factor Correlation Based on the Antoine Equation, Ind & Eng Chem Res.1993;32(1):241-244. https://doi.org/10.1021/ie00013a034.
[50] Shouzhi YI, Yuanyuan JIA, Peisheng MA. Estimation of Acentric Factor of Organic Compounds with Corresponding States Group Contribution Method, Chinese J Chem Eng. 2005;13(5):709-712. http://cjche.cip.com.cn/EN/Y2005/V13/I5/709.

[51] Esfahani RT, Sanjari E. An accurate General Method to Correlate Saturated Vapor Pressure of Pure Substances. Phys Chem Res. 2015;3(1):35-45. https://doi.org/10.22036/pcr.2015.7312.
[52] Grozdani DK. Acentric factor estimation from the corresponding states principle. J Serb Chem Soc. 2006; 71(3):213–221. https://doi.org/10.2298/JSC0603213G.
[53] http://www.coolprop.org/fluid_properties/PurePseudoPure.html
[54] https://www.engineeringtoolbox.com/hydrogen-d_1419.html
[55] https://www.brainkart.com/article/Hydrogen_34702/
[56] Jacobsen RT, Leachman JW, Penoncello SG, Lemmon EW. Current Status of Thermodynamic Properties of Hydrogen, Int J of Thermophys. 2007;28:758–772. https://doi.org/10.1007/s10765-007-0226-7.
[57] Roder HM, Weber LA, Goodwin RD. Thermodynamic and Related Properties of Parahydrogen From the Triple Point to100°K at Pressures to 340 Atmospheres. Library of Congress Catalog Card No.26-60074. National Bureau of Standards Monograph. 1965;94:1-112.
[58] Yaws CL. Chemical Properties Handbook. 1st Edition. McGRAW-HILL Education. New york.1999; 24-29. https://www.accessengineeringlibrary.com/content/book/9780070734012.

Supplementary Files

This is a list of supplementary files associated with this preprint. Click to download.

- Highlights.docx